Available online at www.sciencedirect.com
ScienceDirect
Polymer 48 (2007) 6934–6947
polymer
www.elsevier.com/locate/polymer

Deformation-induced highly oriented and stable mesomorphic phase in quenched isotactic polypropylene

Jie Qiu [a,b], Zhigang Wang [a,*], Ling Yang [c], Junchai Zhao [a], Yanhua Niu [a], Benjamin S. Hsiao [d]

[a] CAS Key Laboratory of Engineering Plastics, Joint Laboratory of Polymer Science and Materials, Beijing National Laboratory for Molecular Sciences, Institute of Chemistry, Chinese Academy of Sciences, Beijing 100080, PR China
[b] Graduate School of Chinese Academy of Sciences, Beijing 100049, PR China
[c] Department of Polymer Science and Engineering, University of Massachusetts, Amherst, MA 01003, USA
[d] Department of Chemistry, Stony Brook University, Stony Brook, NY 11794, USA

Received 7 May 2007; received in revised form 22 July 2007; accepted 31 August 2007
Available online 14 September 2007

Abstract

Changes of structure and morphology of quenched isotactic polypropylene (i-PP) film during tensile deformation at room temperature have been investigated by applying in situ synchrotron small-angle X-ray scattering (SAXS) and wide-angle X-ray diffraction (WAXD) techniques. SAXS patterns show that the isotropic diffuse scattering peak in the initial quenched i-PP film disappears after the film experiences necking and a strong streak, which accompanies obvious film stress-whitening, appears when strain reaches 600% and above. Explanation to the former is the dropping of density contrast between amorphous and mesomorphic phases due to deformation and that to the latter is the formation of microfibrils and/or microvoids in the film. WAXD patterns indicate that i-PP chains in the mesomorphic phase become highly oriented along the drawing direction with the strain value more than 5% and the three-fold helical chain conformation keeps in the deformed mesomorphic phase. The mesomorphic structure in the initial quenched i-PP film does not transform into crystal phase although high orientation appears during tensile deformation and the highly oriented mesomorphic phase is considered to be quite stable. Thermal behaviors of the initial quenched i-PP and deformed i-PP with the strain value of 650% are examined by modulated differential scanning calorimetry (MDSC). MDSC results show that the highly oriented i-PP chains in deformed mesomorphic phase are stable, which brings about restriction to chain mobility and prohibits from phase transformation of mesophase to crystal phase in the temperature range normally measurable for the initial quenched i-PP. A model about tensile deformation of the quenched i-PP is outlined to distinctly illuminate the changes of structure and morphology in both the amorphous and mesomorphic phases.

Keywords: Deformation; Mesomorphic; Isotactic polypropylene

1. Introduction

Mesophase of polymers, especially induced in isotactic polypropylene (i-PP), has attracted extensive attention. Mesomorphic phase which has an intermediate order between the amorphous and crystalline phases has been denoted with different names in the literature: smectic [1,2], paracrystal [6,7], microcrystal [8,9], glass [10], condis crystal [11] or mesomorphic phase [12]. Here we would like to use the terms ''mesomorphic phase'' or ''mesophase'' in this article. In general, two methods can be used to generate mesophase. Quenching the molten polymer at a drastic cooling rate is an effective way to obtain mesophase which can be considered as a ''frozen'' intermediate ordering state during crystallization pathway [11]. It is a consequence of severe solidification condition which prematurely hinders molecular motions necessary for crystallization. Up to now, a great deal of work has been dedicated to this historic mesophase, namely ''quench-induced

* Corresponding author. Tel./fax: +86 10 62558172.
E-mail address: zgwang@iccas.ac.cn (Z. Wang).

0032-3861/$ - see front matter © 2007 Elsevier Ltd. All rights reserved.
doi:10.1016/j.polymer.2007.08.066

mesophase'', in quenched i-PP [1,2,6–19], ethylene/vinyl alcohol copolymers [20], and syndiotactic polypropylene (s-PP) [21,22]. The other kind of mesophase, namely ''deformation-induced mesophase'', can be obtained by processing, commonly, cold-drawing. It is well established that uniaxial tensile test [3–5] is one of the most important experimental methods to characterize the relationship between structure and property, and tensile deformation can generally induce structural evolution of polymers during drawing process [20,23–32]. In some cases, both amorphous and crystalline phases can transform into mesophase during tensile deformation at low temperature. Recently, cold-drawing induced mesophases in amorphous [23,24] or slush [25] poly(ethylene terephthalate), amorphous poly(ethylene naphthalate) [26], amorphous poly(diethylsiloxane) [27,28], crystallized ethylene/vinyl alcohol copolymers [20], crystallized i-PP [29–31], and blends of i-PP and ethylene/propylene copolymer [32] have been found and studied in detail.

i-PP is one of the mostly investigated polymers due to its academic interest and industrial application. i-PP chains can organize into different spatial arrangements giving rise to three basic crystalline polymorphs: α-monoclinic, β-hexagonal, and γ-triclinic phases [2,33–35]. The more interesting finding is that i-PP chains are prone to organize into an arrangement of the mesophase [1,2,6,7], which has an intermediate order between amorphous and crystalline phases. Since Natta et al. reported smectic mesophase of i-PP in 1959 [1], the morphology and property of mesomorphic i-PP have been broadly investigated by using X-ray diffraction, infrared and Raman spectroscopy, electron microscopy, electron diffraction and differential scanning calorimetry (DSC). However, the nature of mesophase is not fully understood yet. It has been widely accepted that the partially ordered mesophase of i-PP is made up of bundles of parallel chains [1,2], which maintain the same three-fold helical conformation just as in the stable α-monoclinic form according to the results of infrared spectra [1,2,6,10], and the long range ordering maintains only along the chain axes, whereas large amounts of disorder in lateral packing are present in small mesomorphic aggregates [1,2]. Corradini et al. [12] compared several models (corresponding to β-hexagonal and α-monoclinic forms, as well as model showing characters of both forms) with the measured WAXD patterns of quenched mesomorphic i-PP and found that the local correlations of chains in quenched i-PP were close to those in α-monoclinic crystals.

Tensile deformation of i-PP has also been investigated extensively because processing conditions strongly affect the morphology and property of i-PP products. Understanding structural deformation during processing is essential for quantitative prediction of product performance. Ran et al. [29,30,32] studied the structure and development of mesophase induced by cold-drawing of crystallized i-PP by synchrotron SAXS and WAXD techniques and found that the mesophase did not show any obvious long range ordering. Stockfleth et al. [36] studied deformation mechanism of oriented crystallized i-PP and PET films under uniaxial stretching by using SAXS, WAXD and birefringence measurements at various temperatures. They interpreted the structural changes by using a lamellar stack model and pointed out the contribution of lamellar separation or lamellar slip depended on strain, temperature and orientation of the stack. AboEIMaaty et al. [37] investigated development of defects in drawn i-PP fibers with an original paracrystalline structure with increasing drawing ratio by using electron microscopy and suggested a simple model to explain the defect formation. Russo and Vittoria [38] determined the intrinsic birefringence of smectic phase during uniaxial stretching and suggested that drawing at room temperature did not allow transformation from smectic phase to crystalline phase. Dasari et al. [39] investigated microstructure evolution of crystallized i-PP from initial surface deformation band to spaced crazes and their inward growth until final fracture as functions of strain and strain rate under uniaxial stretching by using TEM and AFM. Song et al. investigated tensile deformation behaviors of quenched i-PP [40–42] and annealed i-PP [43] by using microscopic infrared dichroism. They studied molecular orientation, disclosed pseudo-affine deformation behavior for the amorphous phase and proposed an interpenetrating network (IPN) model for interpreting the stress–strain relationship of the mesoscale area suffering from necking. Liu et al. [44] studied the yielding behavior of i-PP by using optical microscopy (OM), scanning electron microscopy (SEM), and DSC. Sakuraia et al. [45] investigated effects of molecular weight, molecular weight distribution and isotacticity on the mechanical deformation behaviors of i-PP during hot-drawing by using synchrotron SAXS and WAXD techniques.

It is evident that a great deal of work has been carried out on subjects of mesophase and deformation behaviors of i-PP. However, limited work has been done to comprehensively investigate tensile deformation behavior of mesomorphic i-PP by using in situ synchrotron SAXS and WAXD techniques. In this study, we have found that the WAXD patterns of deformed mesomorphic i-PP obtained by us and other scientists [13,18,46] are quite similar to that of oriented mesomorphic i-PP induced from crystallized i-PP by cold-drawing [29,30], and the long range ordering shown in the initial quenched i-PP (quench-induced mesophase) disappears during tensile deformation. Moreover, the long range ordering could not be found either in the deformation-induced mesomorphic i-PP [29,30]. Therefore, it is quite necessary to clarify the differences among the quench-induced mesophase, deformed mesophase, and deformation-induced mesophase of i-PP.

2. Experimental section

2.1. Sample preparation

In this study, i-PP sample was supplied by ExxonMobil Chemical Company. It had number- and weight-averaged molecular weights, M_n and M_w, of 41,400 and 291,000, respectively, and a polydispersity, M_w/M_n, of 7.0. The melting temperature (T_m) for the i-PP sample was about 164 °C by DSC at a heating rate of 4 °C/min. The initial quenched mesomorphic i-PP films were obtained by fast quenching the i-PP melt on a chill roll set at a temperature of 8 °C from melt extrusion. These films were the samples used as well as in our previous published paper [19]. The estimated quenching

rate was about several hundred degrees centigrade per minute. The film thickness was about 0.08 mm. Rectangular specimens with gauge dimension of 40 mm in length and 9 mm in width were cut out from the film. Two semicircular notches were cut at the edges of the central section of the rectangular specimen in order to initiate an appropriate onset necking position for the film tensile deformation (see the photo image in Fig. 1).

2.2. Tensile deformation procedure

The specimen of i-PP was set in a modified Instron 4410 tensile instrument installed in the path of synchrotron X-ray beam for the in situ tensile deformation study at room temperature. Modification of the Instron instrument allowed the specimen to be symmetrically stretched, which assured that the focused X-ray beam always illuminated at about the same position of the specimen, that was to say, the investigated region on the specimen by X-ray scattering did not shift much due to tensile deformation (see the intersection point of two guidelines in Fig. 1). Besides the data in situ collected by SAXS/WAXD techniques, the changes of stress and strain with time were recorded by the tensile apparatus and the size change of the specimen was recorded by a visual camera during the deformation process. In order to allow data collection using SAXS/WAXD imaging plates in sufficient time, the

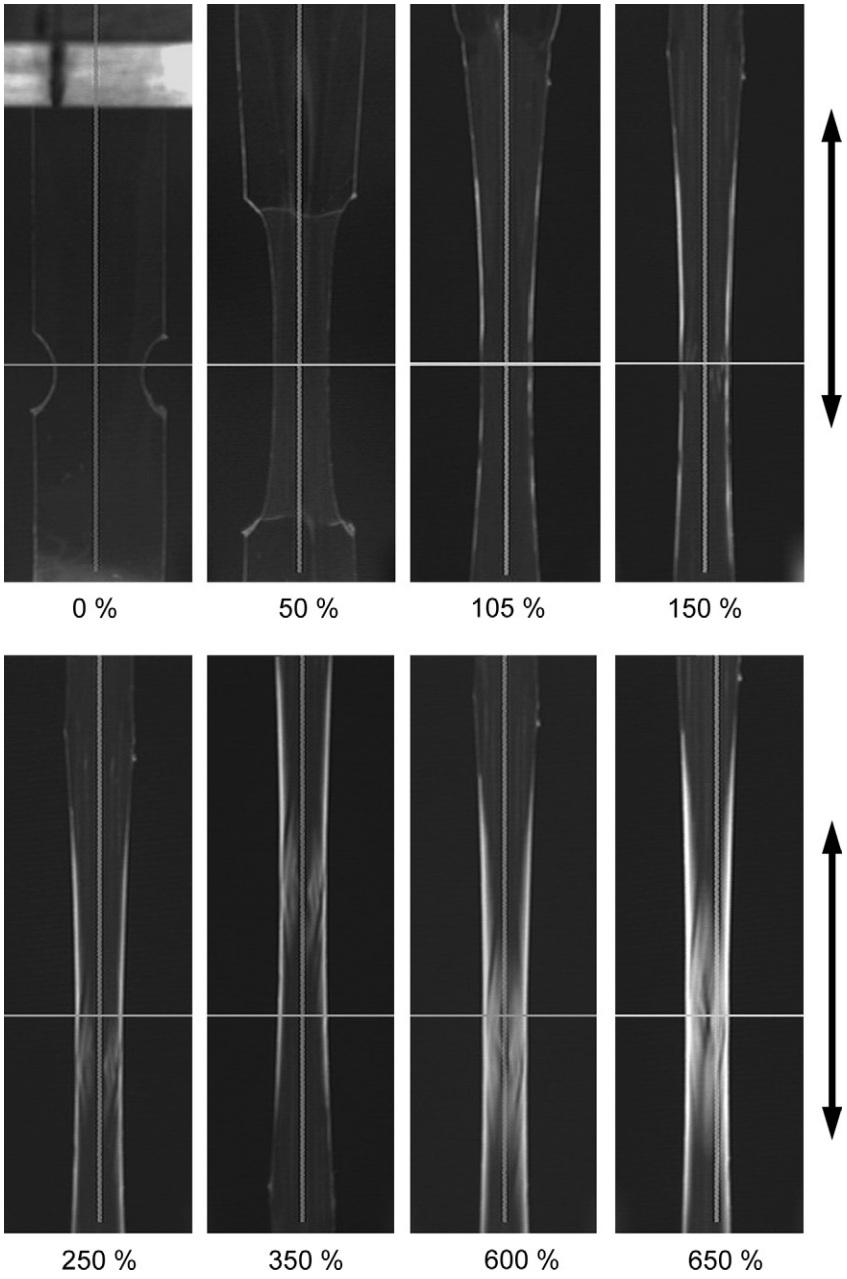

Fig. 1. Photo images of deformed mesomorphic i-PP film during the tensile deformation process at room temperature with the strain values of 0%, 50%, 105%, 150%, 250%, 350%, 600%, and 650%.

sample was drawn stepwise. At each stretching step, the sample was drawn at 4 mm/min. When the strain, ε ($\varepsilon = (l - l_0)/l_0 \times 100\%$, where l_0 is the initial length of the specimen and l is that after deformation) reached a designed value, for example, 50%, SAXS and WAXD patterns were collected for 120 s during which the strain was kept at a constant value and the stress was relaxed. After collection of the SAXS/WAXD patterns, the force was reloaded until the strain reached another larger designed value, namely a new stretching step began. The drawing step was repeated until the strain increased to 650%.

2.3. Synchrotron SAXS/WAXD measurements

Simultaneous SAXS/WAXD measurements were carried out by using two imaging plates at X3A2 Beamline ($\lambda = 1.54$ Å) in the National Synchrotron Light Source (NSLS), Brookhaven National Laboratory (BNL). A three-pinhole collimator system was used to reduce the beam size to 0.6 mm in diameter [47]. The point-focused X-ray beam was aligned perpendicular to the film plane of the specimen. The sample to detector distance was 1235 mm for the SAXS measurement and was 156.2 mm for the WAXD measurement. The acquisition time was 120 s for each SAXS/WAXD patterns.

2.4. Thermal behaviors by modulated DSC (MDSC)

Thermal behaviors of the initial quenched i-PP film and deformed i-PP film with $\varepsilon = 650\%$ were examined by MDSC (Model 2920 DSC from TA Instruments, Newcastle, DE). Two samples of ca. 5 mg were cut from the initial quenched film and from the central stress-whitening area of deformed film with $\varepsilon = 650\%$. The cell constant calibration was performed with an indium standard, and the temperature calibration was obtained with indium and lead metals. A heating rate of 4 °C/min with a modulation amplitude of 0.32 °C in a period of 60 s from −25 °C to 200 °C under nitrogen purge was chosen based upon the recommended specifications given in the instrument manual. The modulation temperature amplitude was smaller relative to the heating rate, so there was no local cooling during the scan, which was referred to as heating-only. The mathematical equation representing DSC heat flow can be expressed as

$$du/dt = C_p(dT/dt) + f(t,T) \quad (1)$$

where u is the amount of heat absorbed by the sample, t the time, C_p the heat capacity of the sample, T the absolute temperature, and $f(t,T)$ the function of time and temperature that governs the kinetics response of any physical or chemical transition. Eq. (1) states that the heat flow of conventional DSC, du/dt, contains two components: one depends on the heating rate (dT/dt) and the other is related to the absolute temperature. It showed that MDSC could separate the total heat flow into the heat capacity-related component (reversible, abbreviated as Rev heat flow) and the kinetics component (nonreversing, abbreviated as Nonrev heat flow). The reversible signal is excellent for quantifying the endothermic melting, while the non-reversible signal contains components of endothermic and exothermic events.

3. Results and discussion

3.1. Film deformation during tensile process

Deformation of the quenched i-PP film during tensile process is displayed in Fig. 1. The arrow on the right side of Fig. 1 denotes the drawing direction. The corresponding strain at each stage is marked below each photo image of the film. It can be seen that the second photo image of the deformed i-PP film with the strain value of 50% in Fig. 1 shows an obvious symmetrical necking, indicating the occurrence of yielding. In fact, on the basis of the stress–time and strain–time curves shown in Fig. 2a and b, it has been found that the deformed i-PP film reaches the yielding point at the strain value of about 5% and the necking is thought to occur at the same moment. Stress-whitening is visible on the edge and in the central area of the deformed i-PP film when the strain reaches 105% and 150%, respectively. Afterwards, the stress-whitening area increases with further increasing strain and covers most of the central part of the deformed i-PP film when the

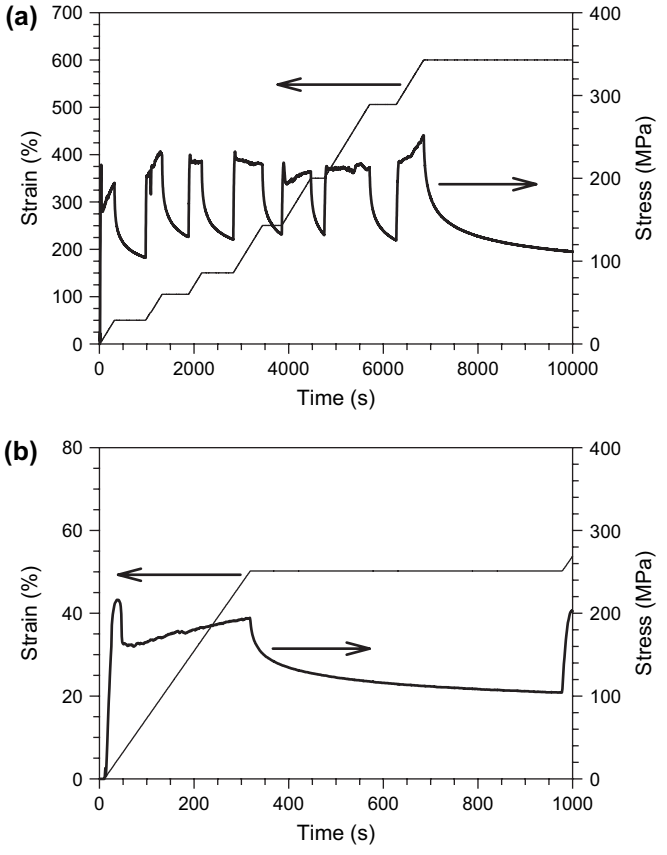

Fig. 2. (a) Strain and stress of the mesomorphic i-PP film as functions of time during the tensile deformation process; (b) enlarged portion of (a) in the initial time period of 1000 s.

strain reaches 600% and above. In general, stress-whitening observed in tensile-deformed polymers is attributed to formation of microfibrils and/or microvoids in the surface and body of the samples [44,48–50]. Here, the appearance of stress-whitening in the necking region of the deformed i-PP film also indicates the formation and growth of microfibrils and/or microvoids.

3.2. Changes of SAXS patterns during tensile process

Two-dimensional (2D) SAXS patterns of the deformed i-PP film collected at different deformation stages are shown in Fig. 3. The arrow at the right bottom corner indicates the drawing direction. The value of strain at each deformation stage is marked on the corresponding SAXS pattern. It can be seen that an isotropic diffuse scattering intensity appears for the initial quenched i-PP film. However, the diffuse scattering intensity of the film decays dramatically at the strain value of 50%, which implies that the partially ordered structures associated with the SAXS pattern in the initial quenched i-PP film vanish or cannot be detected any more by SAXS measurement. In other words, the original ordered microstructures in the quenched i-PP film might be destroyed by tensile deformation or be out of the detection range of the current SAXS measurement setup or the electronic density contrast in the deformed i-PP film just vanishes. Because the corresponding WAXD pattern of the deformed i-PP film, which will be discussed in next section, shows existence of highly oriented mesomorphic structure, the first two reasons to explain the dramatic dropping of diffuse scattering intensity of SAXS can be excluded. The third reason will be further discussed in the later sections. With further increasing strain, there are no obvious changes of the scattering patterns until the strain reaches 600% and above. At the strain value of 600%, a scattering streak on equator can be clearly observed indicating the formation of microfibril structure and/or highly oriented microvoids in the drawing direction [51]. The scattering streak becomes stronger and more distinct with the strain increasing from 600% to 650%. The appearance and development of the scattering streak on equator can be certainly correlated with the stress-whitening phenomenon shown in Fig. 1. It is noticed that for the mesomorphic i-PP film the stress apparently is not homogeneously distributed within the film because the film itself is a heterogeneous system containing the granule-like structure [19] and thus the stress concentrations could possibly, at least partially, lead to the formation of microvoids to give rise to the scattering streak [51].

To compare the long range orderings in the film, it is necessary to examine Lorentz-corrected one-dimensional (1D) SAXS intensity (Iq^2) as a function of the scattering vector q

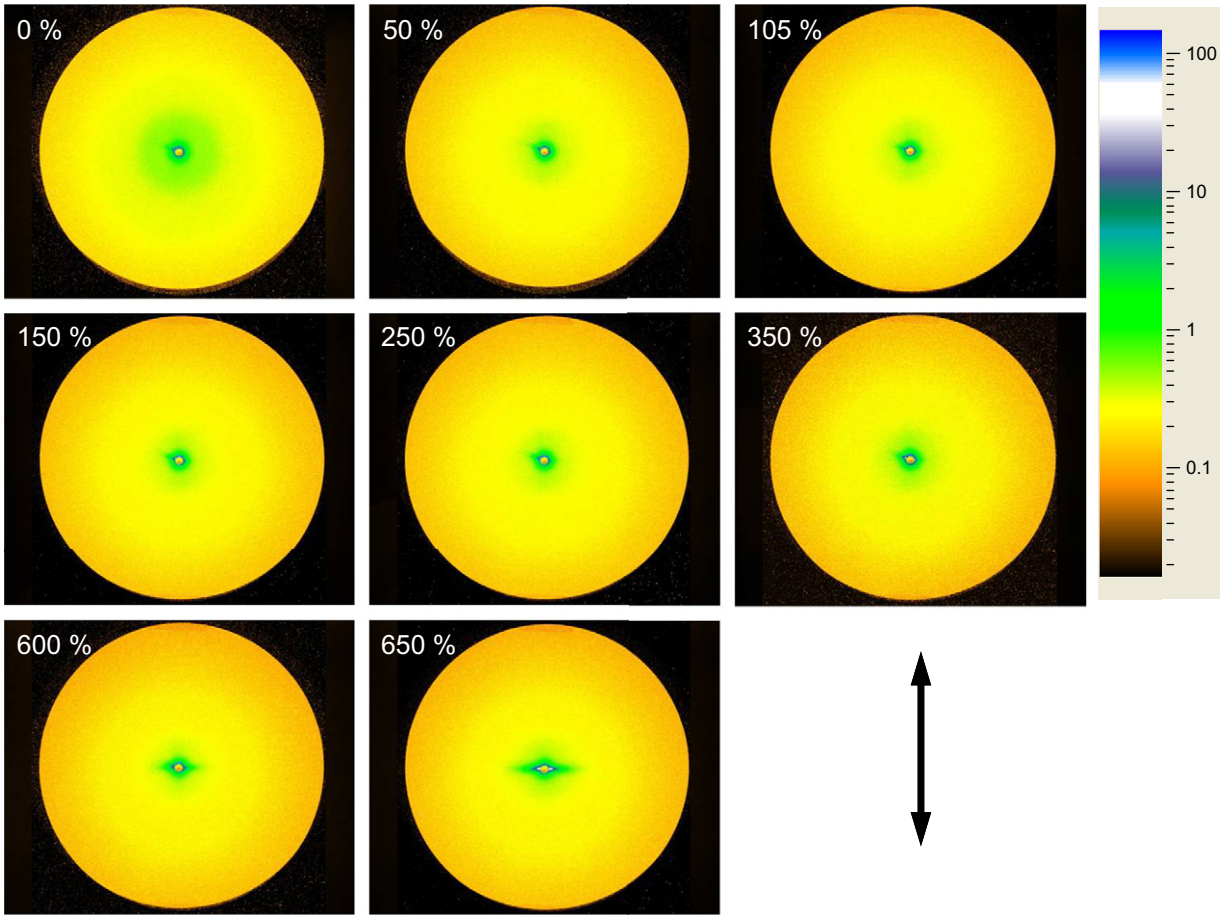

Fig. 3. 2D SAXS patterns of the mesomorphic i-PP film at different strain values during the tensile deformation process.

($q = 4\pi/\lambda \sin\theta$), with λ as the wavelength and 2θ the scattering angle. The results are displayed in Fig. 4. It can be seen that there is a broad scattering peak in the initial quenched i-PP film, while this broad scattering peak is totally absent for all of the deformed i-PP films at different strains. The long range ordering of the embodied clusters or granules in the initial quenched i-PP film can be calculated by using the Bragg's law of $d = 2\pi/q_m$, where q_m is the position of q with the maximum scattering intensity. The q_m locates at about 0.064 $Å^{-1}$, which corresponds to the long range ordering of about 100 Å. This value is in a good agreement with the average adjacent spacing of the clusters or granules, which was previously observed by using TEM method [19]. However, this long range ordering disappeared with strain values of 50% and above, indicating that the effective electronic density contrast between the amorphous and mesomorphic phases vanishes. The mesophase induced in crystallized i-PP by tensile deformation at room temperature neither showed any apparent long range ordering [29,30]. On the basis of the WAXD pattern, Penel et al. [20] found that a mesomorphic-like structure developed from original crystalline phase of ethylene/vinyl alcohol copolymer for the draw temperature below 110 °C and draw ratios beyond $\lambda = 4$ during the tensile-drawing process, and they also found that the sample did not show any SAXS long range ordering. However, they further found that the quench-induced mesomorphic-like structure of ethylene/-vinyl alcohol copolymer neither showed any SAXS long range ordering, which is different from our current experimental result. They interpreted that the absence of SAXS long range ordering was due to similar densities between the mesomorphic and amorphous phases. We may speculate that the chains in the amorphous phase are bound to be elongated along the drawing direction and the chain packing may become tight, resulting in density increasing for the amorphous phase and accordingly the dropping of density contrast between the mesophase and amorphous phase. This should be the main reason for the absence of SAXS long range ordering during deformation in our case.

3.3. Changes of WAXD patterns during tensile process

2D WAXD patterns of the initial quenched i-PP and deformed i-PP are shown in Fig. 5. The arrow at the right bottom corner indicates the drawing direction. The value of strain at each deformation stage is marked on the corresponding WAXD pattern. Two isotropic broad and diffuse diffraction rings can be seen in the WAXD pattern of the initial quenched i-PP. Two broad peaks located at $2\theta = 14.9°$ and 22.0° are seen on the 1D WAXD profile shown in Fig. 6. Appearance of these two isotropic broad diffraction rings or peaks indicates that the quenched i-PP film possesses a mesomorphic structure which organizes with an intermediate order between the amorphous and crystalline phases [1,2,6,7]. There is no measurable orientation in the initial quench-induced mesophase. Compared with the isotropic WAXD pattern of the initial quenched i-PP, two diffraction spots on equator and four weak but distinct off-meridional diffraction arcs on the first layer line appear in the WAXD patterns of the deformed i-PP. In other words, the mesomorphic structure becomes highly orientated during tensile deformation. This phenomenon is consistent with the apparent change of the film when the film necking occurs (Fig. 1). With increasing strain, the azimuthal spread of these off-meridional diffraction arcs becomes narrower and the shape of the diffraction spots on equator gradually changes from round-like to oval-like indicating increasing chain orientation along the drawing direction. This distinct six-point WAXD pattern of the deformed i-PP is usually regarded as the fingerprint of smectic mesophase [18,29,30], although Gezovich and Geil [46] considered that this WAXD pattern could also possibly be indexed as an orientated faulty

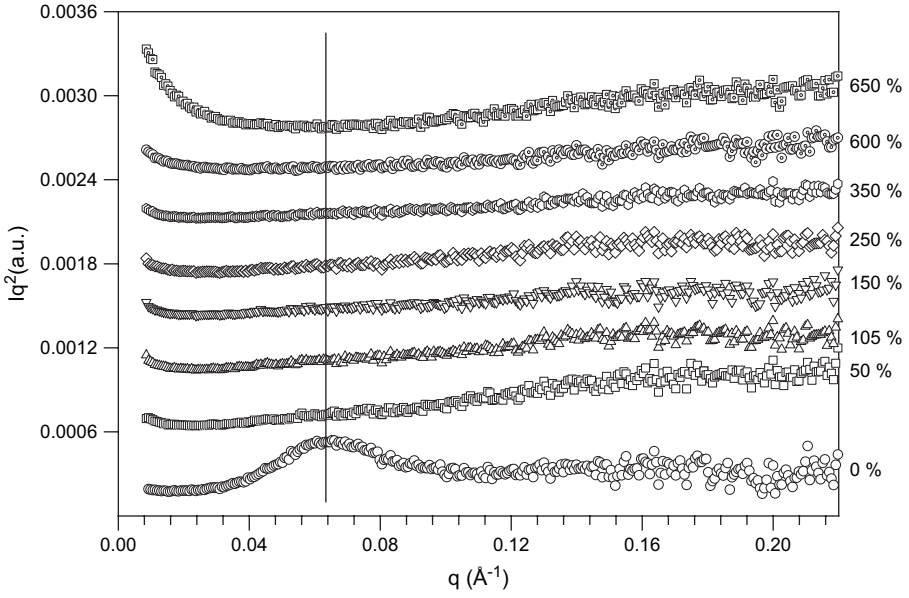

Fig. 4. Lorentz-corrected SAXS intensity profiles of the mesomorphic i-PP film at different strain values during the tensile deformation process.

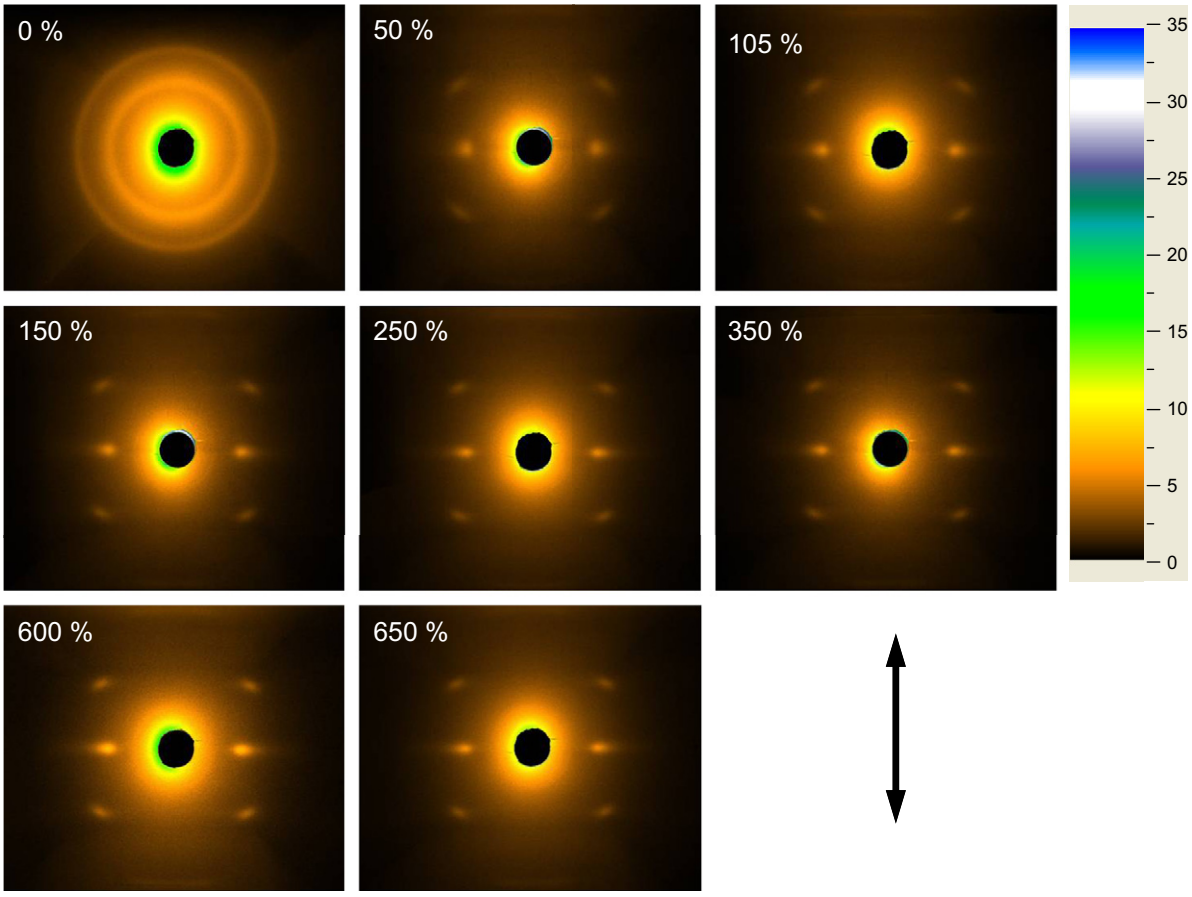

Fig. 5. 2D WAXD patterns of the mesomorphic i-PP film at different strain values during the tensile deformation process.

monoclinic crystal. It has been suggested that drawing the quenched i-PP film at room temperature could not lead to phase transformation from the mesophase to crystalline phase, however, it could produce mesomorphic fibrils [38,54]. Curiously, two additional even broad and weak diffraction arcs on the meridian direction are barely seen in the 2D WAXD

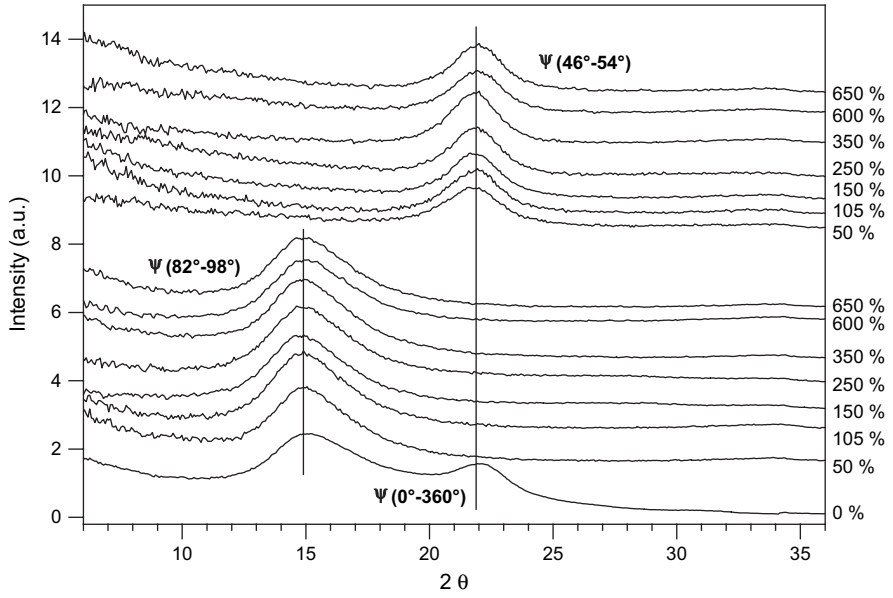

Fig. 6. 1D WAXD intensity profiles of the deformed mesomorphic i-PP film extracted from 2D WAXD patterns by azimuthal averaging from 82° to 98° and from 46° to 54°, respectively, and 1D WAXD intensity profile of the initial quenched mesomorphic i-PP film extracted from 2D WAXD pattern by azimuthal averaging from 0° to 360°. The azimuthal angle starts counterclockwise from the meridian direction.

patterns due to the weak diffraction intensity, but they truly exist and can be indicated by a small peak located at $2\theta = 30.7^\circ$ on the 1D WAXD profiles of the deformed i-PP shown in Fig. 7, which are extracted from the 2D WAXD patterns by azimuthal average scanning on the meridian direction. This type of peak was also observed in the WAXD patterns of tensile-deformed i-PP by other scientists [13,14,29,30], although the peak positions are slightly different due to different used i-PP samples and quench conditions (including cooling rate, quenching reagent, and quenching depth). It is worth noting that the position and intensity of the small peak do not show obvious changes during deformation once it forms. It is believed that its appearance indicates the microstructure change of quench-induced mesophase due to deformation and it may be one of the characters for orientated mesophase. However, the nature of the microstructure change cannot be exactly clarified with the currently available experimental data.

The 1D diffraction intensity−2θ profiles can be extracted from 2D WAXD patterns by azimuthal average scanning from 0° to 360° for the initial quenched i-PP and azimuthal average scanning from 82° to 98° and 46° to 54°, respectively, for the deformed i-PP. Note that the azimuthal angle starts counterclockwise from the meridian direction. The results are displayed in Fig. 6, indicating the existence of two groups of diffraction peaks. McAllister et al. [16] considered that determining precise 2θ value for the first peak was difficult with a diffractometer. Luckily, our experimental 2θ values of 14.9° and 22.0° for the first and second peaks, respectively, were within the ranges summed by them. Miller [6] pointed out that the chains in quenched i-PP had the three-fold helical conformation and the presence of the second peak at about $2\theta = 22.2^\circ$ ($2\theta = 22.0^\circ$ obtained by us) was attributed to the existence of a state of chain aggregation or an intermediate order greater than that attained in atactic PP which was considered to be completely amorphous. Ran et al. [29] suggested that most of the scattered intensity contributed by the orientated mesophase was expected to appear on equator and the scattered intensity on the first layer line was due to the three-fold helical structure. As

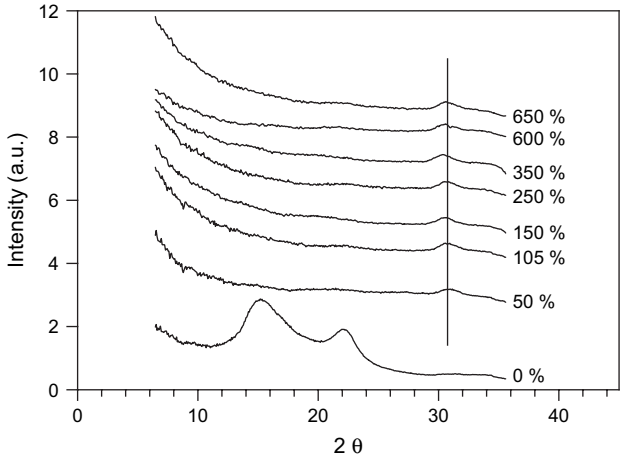

Fig. 7. 1D WAXD intensity profiles extracted from 2D WAXD patterns on the meridian direction for the mesomorphic i-PP film.

concluded in a recent review by Cheng [62], it is well known that the 3_1 helical chains in the crystalline i-PP consist of helical stems which are chiral but racemic and can possess either right or left-handedness. In addition, the methyl groups in crystalline i-PP are tilted to the main chain axis rather than normal to it, which defines 'up' and 'down' orientations of the helices. As a result, i-PP chain has four 3_1 helical conformations with an identical rotational energy in the crystals. During the growth process of α-form crystals, helical chain packing requires the precise arrangement of stems, namely, a right-handed helical stem alternates with left-handed helical stems on the growth front. Moreover, the arrangement of the 'up' and 'down' orientations of the methyl groups leads to two variants of the α-form, the α_1- and α_2-forms. Although the handedness packing in these two sub-forms is identical, the difference is that in the α_1-form, the 'up' and 'down' arrangement is random, while in the α_2-form, it is strictly alternating. Cohen and Saraf [52] considered *c*-axis correlation of the helices, namely, the specific registration of the four types of helices between neighboring chains or stems as the ''inter-chain registration''. In addition, Saraf [31] proposed that the first broad peak for isotropic smectic phase was from the inter-chain lateral packing disorder and the second peak was from the inter-chain registration. Similarly, the equatorial peak for orientated smectic phase corresponds to inter-chain packing and the off-meridional layer line peaks are related to the inter-chain registration [52]. So it is reasonable to suggest the first peak as the signature of chain packing and the second diffraction peak as the signature of three-fold helical structure. In other words, the first broad peak indicates that the lateral packing of helical chains in the mesophase domain is quite disorder [1,2,12] and the second broad peak implies that there is no specific registration for the helical hands of the chains (namely, random assembly of the left or right helical hands [53]). In addition, it is seen that the two groups of diffraction peaks for the deformed i-PP all have lower 2θ values than that of the initial quenched i-PP. The lower 2θ values corresponding to the larger values of the Bragg spacing indicate the increased average inter-chain distances in the deformed i-PP.

3.4. Highly oriented and stable mesomorphic phase during tensile process

Fig. 8a–c shows the azimuthal intensity profiles at three specific 2θ values of 14.9°, 22.0° and 30.7°, respectively. For the 2θ value of 14.9°, corresponding to diffraction spots on equator of the deformed i-PP (Fig. 5), it is clearly seen that there are two groups of relatively sharp peaks at the azimuthal angles (ψ) of 90° and 270°, respectively. Note that only the peak at ψ of 90° is displayed in Fig. 8a. The intensities and positions of these two peaks do not show obvious changes after the film necking during deformation, while the widths of these two peaks show an initial decreasing trend with increasing strain and then show no obvious changes with further increasing strain. This result strongly discloses that the chains in the mesophase domains become highly oriented along the drawing direction and the oriented structures

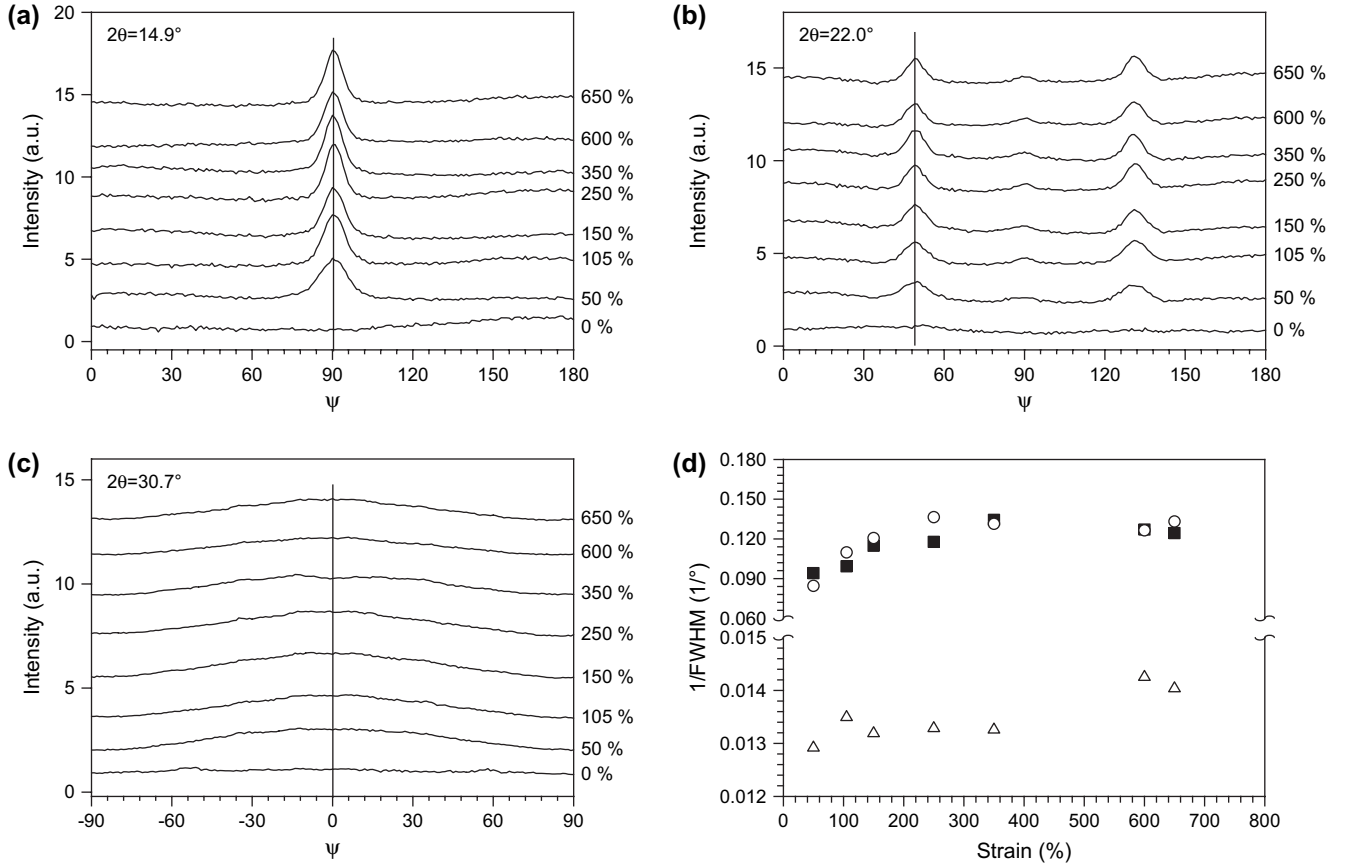

Fig. 8. Azimuthal intensity profiles of the deformed mesomorphic i-PP film at three diffraction angles of (a) 14.9°, (b) 22.0° and (c) 30.7°; (d) changes of value of reversing FWHM with strain for the three different diffraction angles, ○ 14.9°, ■ 22.0° and △ 30.7°.

are stable once the strain passes over the yielding point for film necking. For the 2θ value of 22.0°, corresponding to the four off-meridional diffraction arcs of the deformed i-PP (Fig. 5), it is clearly seen that there are four groups of relatively broad peaks at the azimuthal angles (ψ) of 50°, 130°, 230° and 310°. Note that only the peaks at ψ of 50° and 130° are displayed in Fig. 8b. The intensities and positions of these four peaks do not change obviously during deformation, while the widths of these four peaks show an initial decreasing trend with increasing strain and then show no obvious changes with further increasing strain, which reveals that the chains adopting the three-fold helical conformation in the mesophase domains become stable beyond the yielding point for film necking and the chains are highly oriented when the degree of orientation is prone to saturate. For the 2θ value of 30.7°, two groups of much broad and much weak peaks on the azimuthal intensity profiles, possibly denoting the relatively weak orientation of the tie molecules between the mesophase domains, can be found to locate at $\psi = 0°$ and 180°, respectively. Note that only the peak at ψ of 0° is displayed in Fig. 8c. The intensities and positions of these two peaks do not change obviously during deformation, while the widths of these two peaks show a decreasing trend with increasing strain.

To quantitatively represent the change of the degree of orientation for the mesomorphic phase during deformation, the reverse of the full width half-maximum (FWHM) of the particular peak on the azimuthal intensity profile was obtained for each particular diffraction angle. The results are shown in Fig. 8d. The inverses of the determined FWHM values are plotted as functions of strain for the 2θ values of 14.9°, 22.0° and 30.7°. Changes of the degree of orientation can be easily found in Fig. 8d. For the 2θ values of 14.9° and 22.0°, the degree of orientation increases rapidly after yielding point for film necking with increasing strain up to the strain value of about 250%, then the degree of orientation does not change obviously with further increasing strain. For these two diffraction angles, changes of the degree of orientation almost follow the same trend. For the 2θ value of 30.7°, the degree of orientation seems to increase constantly with increasing strain up to the strain value of about 650%. The degree of orientation corresponding to $2\theta = 30.7°$ is much lower than those corresponding to $2\theta = 14.9°$ and $2\theta = 22.0°$.

The above results further prove that the chains in the mesophase domains are highly oriented and the degree of orientation is prone to be stable beyond the strain value of 50%. Parthasarthy et al. [54] investigated the deformation behavior of quenched i-PP by using rheoptical Fourier transform infrared (FTIR) spectrometer. Their results also showed the similar phenomenon that the orientation of ‘‘crystalline regions’’ (that is the mesomorphic region) was prone to saturate just beyond the yielding point, whereas the majority of post-yielding

orientation occurred in the amorphous region. They suggested that the smectic crystallites commenced the irreversible deformation via the slip and dislocation movements beyond the yielding point and the chains in the amorphous region began to undergo elongation and continued to behave so until material failure, accompanying a continuous increase in orientation. In addition, they proposed that the smectic crystallites did not transform into the α-form monoclinic crystals, even at the strain value of 250% at room temperature. It is obvious that their results are consistent with ours. Therefore, it can be considered that the amorphous phase suffers from an affine deformation and the mesophase domains embedded in the amorphous matrix are induced to rotate accompanying partial elongation of the amorphous chains before yielding point. As a result, most of the mesophase domains may align along the drawing direction and the chains in the mesophase domains become highly orientated near the yielding point, whereas the amorphous chains may be continuously elongated until film failure.

3.5. Thermal behavior associated with tensile deformation

It is predicted that the highly oriented mesophase in deformed i-PP is stable and it cannot relax to recover to its isotropic mesomorphic state when the loading force is released. Thus, the highly oriented and stable mesophase could show obvious influences on thermal behavior of deformed i-PP film. On the other hand, the thermal behavior of deformed i-PP film could be also possibly used to indicate the highly oriented and stable mesomorphic morphology in the film. To confirm the above prediction, MDSC measurements were performed. Fig. 9a shows the total heat flow curves of MDSC scans at a heating rate of 4 °C/min for the initial quenched i-PP film with the strain value of 0% and deformed i-PP film with the strain value of 650%. The total heat flow curve of the initial quenched i-PP film shows two endothermic peaks (Endo 1 and Endo 2, indicated in Fig. 9a) and one exothermic peak (Exo, indicated in Fig. 9a). The occurrence of the small and broad endothermic peak (Endo 1, peak temperature of 61.5 °C and enthalpy of 11.4 J/g) located in the lower temperature range is ascribed to the melting of the mesophase. The small and broad exothermic peak (Exo, peak temperature of 97.5 °C and enthalpy of 3.9 J/g) in the intermediate temperature range corresponds to the recrystallization process of the melted mesophase to form α-form monoclinic crystal phase. The large and sharp endothermic peak (Endo 2, peak temperature of 162.3 °C and enthalpy of 109.0 J/g) in the higher temperature range is consistent with the melting and recrystallization behavior of α-form monoclinic crystals. The true

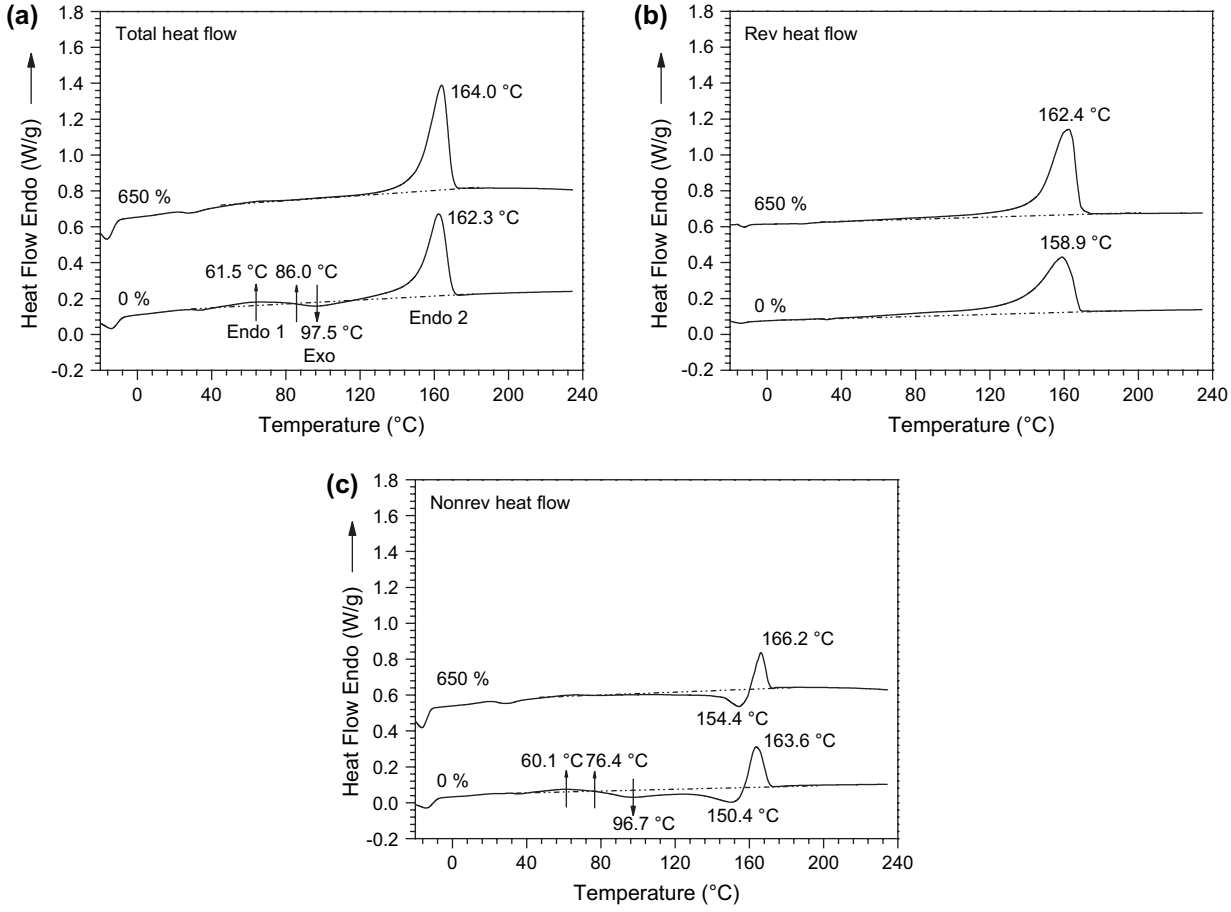

Fig. 9. MDSC heat flow curves of the mesomorphic i-PP films with strains of 0% and 650%. MDSC heating rate is 4 °C/min with a modulation amplitude of 0.32 °C in a period of 60 s. (a) total heat flow; (b) reversible heat flow; (c) nonreversing heat flow.

magnitudes of heat flow related to both the small endothermic and exothermic peaks might be larger than the apparently detected total heat flow values due to the possible superposition of the two physical transitions with opposite signs. This viewpoint can be easily verified by the comparison between the reversible and nonreversing heat flow curves from MDSC measurements. The reversible heat flow curve of the initial quenched i-PP film shown in Fig. 9b indicates that the continuous melting behavior starts as early as above 60 °C (Endo 2, peak temperature of 158.9 °C and enthalpy of 130.2 J/g). The nonreversing heat flow curve of the initial quenched i-PP film shown in Fig. 9c indicates that the exothermic peak (Exo, peak temperatures of 96.7 °C and 150.4 °C and enthalpy of 46.0 J/g) is more significant than that in Fig. 9a, inferring that the more significant mesomorphic phase transformation (from mesophase to crystal phase) or recrystallization behaviors truly occur during the heating process. The above results are consistent with our previous report in Ref. [19] and provide more information to support the phase transformation viewpoint related to the mesomorphic i-PP.

However, on the total heat flow curve of deformed i-PP film with the strain value of 650% shown in Fig. 9a, only one large and sharp endothermic peak in the higher temperature range appears and its peak temperature of 164.0 °C and enthalpy of 139.0 J/g are higher than that of the initial quenched i-PP film. The reversible heat flow curve of deformed i-PP film shown in Fig. 9b indicates that the continuous melting behavior starts as early as above 90 °C and its peak temperature of 162.4 °C and enthalpy of 140.5 J/g are also higher than that of the initial quenched i-PP film. The nonreversing heat flow curve of deformed i-PP film shown in Fig. 9c indicates that the exothermic peak (Exo, peak temperature of 154.4 °C and enthalpy of 25.4 J/g) appears in much higher temperature range (above 110 °C and up to 160 °C), inferring that it is more related to the general melting and recrystallization behavior for i-PP rather than the mesomorphic phase transformation behavior for mesomorphic i-PP. The absence of mesomorphic phase transformation in deformed i-PP film in MDSC measurement might be explained as follows. Compared with isotropic mesomorphic i-PP, deformed mesomorphic i-PP contains highly oriented chains, which restrain molecular chain mobility in both the amorphous and mesomorphic phases [55]. The highly oriented mesomorphic phase also becomes stable. The restrained molecular chain mobility may prohibit from the reorganization of the oriented mesophase into α-form monoclinic crystal at lower temperatures, and consequently the ‘‘melting’’ of the highly oriented mesophase, if it does happen, may shift to higher temperatures. The increase of ‘‘melting point’’ of the highly oriented and stable mesomorphic phase may lead to its melting to combine with the general melting of i-PP crystals, that is to say, resulting in the only endothermic peak shown in Fig. 9b (heat flow curve for 650%) and its recrystallization thus may also happen in a similar higher temperature range for i-PP crystals, resulting in the only exothermic peak shown in Fig. 9c (heat flow curve for 650%). The highly oriented and stable mesomorphic phase may not completely melt before the recrystallization events occur and may serve to induce recrystallization for both the amorphous i-PP and partially molten mesomorphic i-PP components. It has also been found that the monoclinic crystals of i-PP annealed from oriented mesophase still contain highly oriented chains [13,52]. The orientation-induced crystallization can certainly improve the melting point. As proved from Fig. 9, the α-form monoclinic crystals in the deformed i-PP film melt at higher temperature than the isotropic α-form crystals in the undeformed film. In summary, thermal behaviors of deformed i-PP film from MSDC measurements indicate that the highly oriented mesomorphic phase is stable and can only be melted at high enough temperatures compared with the isotropic mesomorphic phase. Table 1 summarizes the peak temperatures and the enthalpies of endothermic and exothermic peaks for the initial quenched (strain of 0%) and deformed (strain of 650%) i-PP films from the MDSC measurements.

3.6. Model and mechanism about deformation of mesophase

Semicrystalline polymer deformation has been widely investigated. Up to now, two mechanisms about deformation are commonly accepted. One is the microfibril model proposed by Peterlin [56]. This model describes the fragmentation of spherulitic crystals, breakup of lamellae, and reorganization of chains pulled out from initial crystals to form microfibrils. The other one proposes that crystalline lamellae may locally melt under tension and then the molten chains recrystallize into an oriented fibril structure. However, the deformation mechanism for mesomorphic quenched i-PP film might be different from that of the crystallized i-PP samples [46]. In contrast to the affine deformation observed in quenched i-PP film, crystallized i-PP films show a complete destruction of the internal organization of the spherulites when drawn at room temperature [46]. In this study, a simple model is suggested to describe the deformation of quenched i-PP. The model is schematically illustrated in Fig. 10. The quench-induced mesomorphic i-PP film contains partially ordered phase which is made up of bundles of parallel chain segments with the three-fold helical conformation and overall shows a granular structure [15]. The granule structure stands for the mesophase domain which embeds in the amorphous matrix of random coils

Table 1
Peak temperatures and enthalpies of endothermic and exothermic peaks for the initial quenched (strain of 0%) and deformed (strain of 650%) i-PP films from the MDSC measurements

		Endo 1	Exo	Endo 2
0%	Total	61.5 °C, 11.4 J/g	97.5 °C, −3.9 J/g	162.3 °C, 109.0 J/g
	Rev	–	–	158.9 °C, 130.2 J/g
	Nonrev	60.1 °C, 4.9 J/g	96.7 °C/150.4 °C, −46.0 J/g	163.6 °C, 27.9 J/g
650%	Total	–	–	164.0 °C, 139.0 J/g
	Rev	–	–	162.4 °C, 140.5 J/g
	Nonrev	–	154.4 °C, −25.4 J/g	166.2 °C, 23.5 J/g

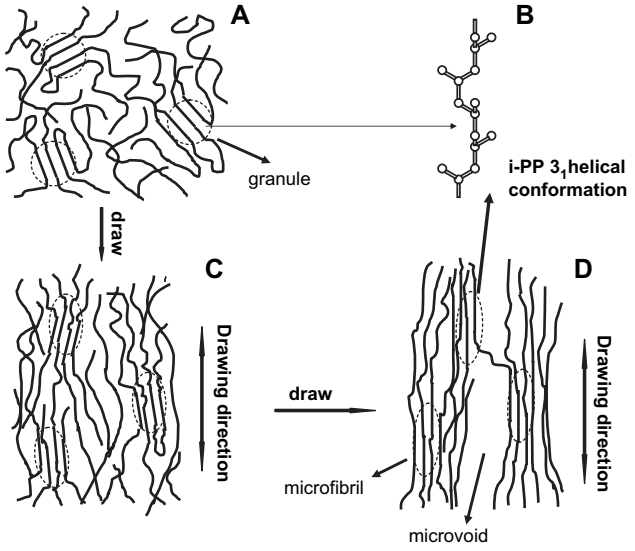

Fig. 10. Schematic model for the quenched mesomorphic i-PP and its deformation. (A) Initial quenched mesomorphic i-PP with granular-like structure; (B) three-fold helical conformation of the chains in the granules; (C) structure changes in the early stage of deformation; (D) formation of microfibrils and/or microvoids in the late stage of deformation.

(Fig. 10A and B). When a force is loaded to the film, the mesophase domains are induced to rotate accompanying partial elongation of the amorphous chains and become highly oriented when the film reaches the yielding point for necking (Fig. 10C). As a result, the chains in both the mesophase domain and amorphous phase become highly oriented even though the chains in the latter are less orientated than that in the former [38,41,42,54]. Orientation of chains in the mesophase domains is prone to saturate when the strain value is 50% and above. At the meanwhile, the partial elongation and orientation of the chains in the amorphous phase lead to tight chain packing to increase the density of the amorphous phase. Upon loading, the chains in the mesophase domains may slip and dislocate along the drawing direction, resulting in insertion of partial amorphous chains into the mesophase domain and/or removing partial parallel chains from the mesophase into the amorphous phase, which bring out slight increase of inter-chain distance and decrease the density of the mesophase (Fig. 10D). Thus, the density contrast between the amorphous phase and mesophase decreases. Accompanying further increasing strain, more amorphous chains will be unfolded and oriented along the drawing direction and reorganize to microfibrils, which are connected together with the highly oriented mesomorphic bundles by the tie molecules. Furthermore, tight packing of the extended chains also stimulates the formation and growth of microvoids along the drawing direction (Fig. 10D). The microfibrils and/or microvoids can give rise to the SAXS streak on equator (Fig. 3).

3.7. Difference between quench-induced mesophase and deformation-induced mesophase

It is obvious that the mesophase formed during tensile deformation of crystallized i-PP is different from the mesophase produced by quenching the molten i-PP to a low temperature although the former is similar to the deformed one of the latter according to the results of SAXS and WAXD measurements from us and other scientists [13,18,29,30,45]. Formation of the former is a process from order to disorder, while that of the latter is from disorder to ''order''. Deformation-induced mesophase from crystalline polymer may undergo a two-step process: at first, the helices are ''unraveled'' or pulled out from crystal lamellae; then, these extended helical chains reorganize to form the mesophase. In other words, the formation of deformation-induced mesophase is ascribed to unfolding and orientation, leading to the formation of an intermediate order. The formation of quench-induced mesophase takes another way. During the fast cooling, the chains undergo a conformational ordering from random coil to three-fold helix, but the packing of helices is not as so well organized as in the α-form monoclinic crystal phase. It results from the fact that the conformational changes can occur rapidly, but the ordered lateral packing requires strict correlation of handedness and direction of the adjacent helices. It may require long range rearrangements to accomplish the inter-chain packing process [52]. Therefore, the formation of quench-induced mesophase is due to the ''pause'' of potential crystallization. Typically, it is understood that the obvious difference between these two processes is that the deformation-induced mesophase is highly oriented rather than isotropic, while the quench-induced mesophase can be isotropic without any orientation.

The structure and morphology of quench-induced mesophase have been widely studied. Early electron microscopic studies by Gezovich and Geil [15] revealed the nodular (granular) structure (125 Å in diameter) in quenched i-PP film and they suggested that there was ''granular-like'' structure which had small and imperfect hexagonal crystallites in the film. Gailey and Ralston [14] found that the partially ordered phase was composed of small hexagonal crystals (50–100 Å in diameter) by WAXD. McAllister et al. [16] found that the chain helices in quenched i-PP were arranged in a square array and the crystallite sizes calculated by using Scherrer equation were approximately 30 Å. Caldas et al. [57] suggested that the microcrystalline regions in quenched i-PP had sizes from 100 Å to 200 Å by using scanning transmission electron microscopy. It is clearly inferred that the sizes of the ''granular structure'' in the quenched i-PP obtained by different scientists change in a wide range due to the different quench conditions and different applied experimental techniques. In general, it is thought that the SAXS peak is brought about by density fluctuations at the order of 80–200 Å [47]. Some of the quench-induced mesophase may not have the ''SAXS long range order'' [58,59], whereas others may show weak diffuse scattering peak in 2D SAXS pattern and have the Bragg long periods [54,60]. In this study, the diffuse scattering peak has been observed, which corresponds to the Bragg long period of about 100 Å. The Bragg long period is in a good agreement with the average adjacent spacing of the clusters, observed by TEM [19]. However, it has also been found that the deformation-induced mesophase does not show any obvious SAXS long range order [20,29,30,32]. The main reason to the

absence of the ''SAXS long range order'' in the oriented mesophase has been given in the previous sections in which the dropping of density contrast between amorphous phase and mesophase is described. It is worth noting that the shear displacement and dislocation of chains in the mesophase may blur the boundary between amorphous phase and mesophase, which may also decrease the density contrast between amorphous phase and mesophase. Such a viewpoint was once used to explain the disappearance of the meridional SAXS peak during drawing process for fibrous material [61]. As a summary, the quench-induced mesophase may show the ''SAXS long range order'' if the mesophase domains are within the right size range for the SAXS measurement setup, however, the deformation-induced mesophase which is similar to the deformed quench-induced mesophase usually does not show the ''SAXS long range order'' at the similar measurement conditions due to the weak density contrast between the oriented amorphous phase and mesophase.

4. Conclusions

Changes of structure and morphology of quenched mesomorphic i-PP film during the deformation process at room temperature have been studied by using in situ synchrotron SAXS/WAXD techniques. Thermal behaviors of the initial quenched i-PP and deformed i-PP films have been examined by using modulated DSC. For the quenched i-PP film the WAXD pattern indicates existence of an isotropic mesomorphic phase with no orientation and the SAXS pattern indicates existence of a long range order of about 100 Å. The chains in the mesophase domains become highly oriented while keeping the three-fold helical conformation when the i-PP film passes through the yielding point for film necking. The degree of orientation is prone to saturate beyond the strain value of 5%. When the strain reaches 600% and above, stress-whitening of the film can be obviously observed with the SAXS pattern showing a strong scattering streak on equator, indicating the formation of microfibril structure and/or microvoids. The SAXS isotropic diffuse scattering peak observed in the initial quenched i-PP disappears after film necking. The absence of the SAXS long range ordering is mainly due to the dropping of density contrast between the amorphous phase and mesophase during deformation. The deformed quench-induced mesophase of i-PP might be relatively similar to the deformation-induced mesophase from crystallized i-PP according to the results of SAXS and WAXD measurements. However, they are essentially different because the latter is highly oriented with no SAXS long range ordering while the former can be isotropic with an obvious SAXS long range ordering. The total heat flow curve of the initial quenched i-PP film in the MDSC measurement shows three obvious transitions, indicating the melting of mesophase, reorganization of the molten mesophase to form α-form monoclinic crystals and the melting of α-form monoclinic crystals, respectively. These three transitions can be further verified by the reversible and nonreversing heat flows. However, the total heat flow curve of deformed mesomorphic i-PP with the strain value of 650% only displays one transition of the melting of α-form monoclinic crystals, which occurs in the relatively higher temperature range. Thermal behavior of the deformed i-PP film indicates that the highly oriented mesomorphic phase obtained by tensile deformation of quenched i-PP is stable and can only be melted at high enough temperatures compared with the isotropic mesomorphic phase.

Acknowledgements

Z.G. Wang thanks financial supports from ''One Hundred Young Talents'' Program of Chinese Academy of Sciences, National Science Foundation of China with Grant no. 10590355 for the Key Project on Evolution of Structure and Morphology during Polymer Processing, and National Science Foundation of China with Grant no. 20674092.

References

[1] Natta G, Peraldo M, Corradini P. Rend Accad Naz Lincei 1959;26:14.
[2] Natta G, Corradini P. Nuovo Cimento Suppl 1960;15:40.
[3] Nitta K-H, Shin Y-W, Hashiguchi H, Tanimoto S, Terano M. Polymer 2005;46:965.
[4] Benetti EM, Causin V, Marega C, Marigo A, Ferrara G, Ferraro A, et al. Polymer 2005;46:8275.
[5] Arranz-Andrés J, Guevara JL, Velilla T, Quijada R, Benavente R, Pérez E, et al. Polymer 2005;46:12287.
[6] Miller RL. Polymer 1960;1:135.
[7] Hosemann R. Acta Crystallogr 1951;4:520.
[8] Bodor G, Grell M, Kallo A. Faserforsch Textil-Tech 1964;15:527.
[9] Farrow G. J Appl Polym Sci 1965;9:1227.
[10] Glotin M, Rahalkar RR, Hendra PJ, Cudby MEA, Willis HA. Polymer 1981;22:731.
[11] Gerbowicz J, Lau SF, Wunderlich B. J Polym Sci Polym Symp 1984;71:19.
[12] Corradini P, Petraccone V, de Rosa C, Guerra G. Macromolecules 1986;19:2699.
[13] Wyckoff HW. J Polym Sci 1962;62:83.
[14] Gailey JA, Ralston PH. Plast Eng Trans 1964;4:29.
[15] Gezovich DM, Geil PH. Polym Eng Sci 1968;8:202.
[16] McAllister PB, Carter TJ, Hinde RM. J Polym Sci Polym Phys Ed 1978;16:49.
[17] Lee S, Miyaji H, Geil PH. J Macromol Sci Phys 1983;B22:489.
[18] de Candia F, Iannelli P, Staulo G, Vittoria V. Colloid Polym Sci 1988;266:608.
[19] Wang ZG, Hsiao BS, Srinivas S, Brown GM, Tsou AH, Cheng SZD, et al. Polymer 2001;42:7561.
[20] Penel L, Djezzar K, Lefebvre J-M, Seguela R, Fontaine H. Polymer 1998;39:4279.
[21] Nakaoki T, Ohira Y, Hayashi H, Horii F. Macromolecules 1998;31:2705.
[22] Vittoria V, Guadagno L, Comotti A, Simonutti R, Auriemma F, de Rosa C. Macromolecules 2000;33:6200.
[23] Ran S, Wang ZG, Burger C, Chu B, Hsiao BS. Macromolecules 2002;35:10102.
[24] Kawakami D, Ran S, Burger C, Fu B, Sics I, Hsiao BS. Macromolecules 2003;36:9275.
[25] Kawakami D, Hsiao BS, Burger C, Ran S, Avila-Orta C, Sics I, et al. Macromolecules 2005;38:91.
[26] García Gutiérrez MC, Karger-Kocsis J, Riekel C. Macromolecules 2002;35:7320.
[27] Hedden RC, Tachibana H, Duncan TM, Cohen C. Macromolecules 2001;34:5540.
[28] Koerner H, Luo Y, Li X, Cohen C, Hedden RC, Ober CK. Macromolecules 2003;36:1975.

[29] Ran S, Zong X, Fang D, Hsiao BS, Chu B, Phillips RA. Macromolecules 2001;34:2569.
[30] Ran S, Zong X, Fang D, Hsiao BS, Chu B, Cunniff PM, et al. J Mater Sci 2001;36:3071.
[31] Saraf RF. Polymer 1994;35:1359.
[32] Ran S, Hsiao BS, Agarwal PK, Varma-Nair M. Polymer 2003;44:2385.
[33] Turner-Jones A, Cobbold AJ. J Polym Sci 1968;B6:539.
[34] Mencik Z. J Macromol Sci Phys 1972;B6:101.
[35] Meille SV, Bruckner S, Porzio W. Macromolecules 1990;23:4114.
[36] Stockfleth J, Salamon L, Hinrichsen G. Colloid Polym Sci 1993;271:423.
[37] AboEIMaaty MI, Bassett DC, Olley RH, Dobb MG, Tomka JG, Wang IC. Polymer 1996;37:213.
[38] Russo R, Vittoria V. J Appl Polym Sci 1996;60:955.
[39] Dasari A, Rohrmann J, Misra RDK. Mater Sci Eng A 2003;358:372.
[40] Song Y, Nitta K-H, Nemoto N. Macromolecules 2003;36:1955.
[41] Song Y, Nitta K-H, Nemoto N. Macromolecules 2003;36:8066.
[42] Song Y, Nemoto N. Polymer 2005;46:6522.
[43] Song Y, Nemoto N. Polymer 2006;47:489.
[44] Liu Y, Truss RW. J Polym Sci Part B Polym Phys 1994;32:2037.
[45] Sakurai T, Nozue Y, Kasahara T, Mizunuma K, Yamaguchi N, Tashiro K, et al. Polymer 2005;46:8846.
[46] Gezovich DM, Geil PH. Polym Eng Sci 1968;8:210.
[47] Chu B, Hsiao BS. Chem Rev 2001;101:1727.
[48] Srinivas S, Brant P, Huang Y, Paul DR. Polym Eng Sci 2003;43:831.
[49] Dasari A, Misra RDK. Acta Mater 2004;52:1683.
[50] Hadal R, Yuan Q, Jog JP, Misra RDK. Mater Sci Eng A 2006;418:268.
[51] Pawlak A, Galeski A. Macromolecules 2005;38:9688.
[52] Cohen Y, Saraf RF. Polymer 2001;42:5865.
[53] Lotz B. Eur Phys J E 2000;3:185.
[54] Parthasarthy G, Sevegney M, Kannan RM. J Polym Sci Part B Polym Phys 2002;40:2539.
[55] Peterlin A. J Polym Sci Part C 1967;15:337.
[56] Peterlin A. J Mater Sci 1971;6:490.
[57] Caldas V, Brown GR, Nohr RS, MacDonald JG, Roboin LE. Polymer 1994;35:899.
[58] Hsu CC, Geil PH, Miyaji H, Asai K. J Polym Sci Part B Polym Phys 1986;24:2379.
[59] O'Kane WJ, Young RJ, Ryan AJ, Bras W, Derbyshire GE, Mant GR. Polymer 1994;35:1352.
[60] Martorana A, Piccarolo S, Sapoundjieva D. Macromol Chem Phys 1999;200:531.
[61] Peterlin A. J Appl Phys 1977;48:4099.
[62] Cheng SZD, Lotz B. Polymer 2005;46:8662.